Asian Journal of Current Research in Clinical Cancer
ISSN: 3062-4444
2025, Volume 5, Issue 1, Page No: 157-176

Available online at: www.galaxypub.co/page/journals

Galaxy Publication

Galaxy Publication

S6K1 Amplification Drives Primary Resistance to CDK4/6 Inhibitors via c-Myc Pathway Activation in Estrogen Receptor–Positive Breast Cancer

Jun M. Miller[1], Kenji C. Fernandez[1], Paolo I. Moore[1], Omar G. Smith[1], Anna Sharma[1]*, Andrew Tanaka[1]

[1]Department of Clinical Cancer Research, Faculty of Medicine, KU Leuven, Leuven, Belgium.

***E-mail** ✉ asharma@hotmail.com

Received: 01 November 2024; **Revised:** 29 January 2025; **Accepted:** 02 February 2025

ABSTRACT

The combination of CDK4/6 inhibitors and endocrine therapy is now the standard first-line treatment for estrogen receptor-positive (ER+) metastatic breast cancer. Despite this, biomarkers predicting primary resistance to CDK4/6 inhibitors and the underlying mechanisms are still poorly understood. This study aimed to identify key molecular features and potential therapeutic targets associated with primary resistance to these inhibitors. An initial cohort of 36 patients treated with palbociclib plus endocrine therapy served as the discovery group. Next-generation sequencing of circulating tumor DNA (ctDNA) from these individuals was conducted to detect genomic changes linked to primary resistance to palbociclib. The identified potential biomarker was subsequently confirmed in a separate validation cohort of 104 patients, as well as in external public datasets. Functional validation of resistance was performed using parental MCF-7 and T47D cell lines, along with modified versions created via small interfering RNA knockdown and lentiviral overexpression. Underlying mechanisms were explored through RNA sequencing, chromatin immunoprecipitation, and reporter gene assays. The efficacy of targeted combination therapies was assessed in patient-derived organoids and xenograft models. Within the discovery group, amplification of S6K1 (observed in 3/35 cases, approximately 9%) emerged as a significant factor contributing to primary resistance against CDK4/6 inhibition. In the validation cohort, elevated S6K1 expression was detected in 15/104 patients (14%). Among those treated with palbociclib, individuals with high S6K1 levels exhibited markedly shorter progression-free survival compared to those with low expression (hazard ratio = 3.0, P = 0.0072). Analysis of aggregated public datasets indicated that S6K1 amplification occurs in about 12% of breast cancer cases overall. Furthermore, elevated S6K1 expression in breast cancer was associated with reduced relapse-free survival (hazard ratio = 1.31, P < 0.0001). In experimental models, S6K1 overexpression driven by gene amplification alone was capable of inducing palbociclib resistance in breast cancer cells. This effect was mediated primarily by upregulation of proteins involved in G1-to-S phase progression and enhanced Rb phosphorylation, largely via activation of the c-Myc signaling pathway. Importantly, co-treatment with an mTOR inhibitor, which targets the pathway upstream of S6K1, effectively reversed this resistance both in cell-based assays and animal models. Amplification of S6K1 represents a key driver of primary resistance to palbociclib in breast cancer. Patients harboring S6K1-amplified tumors may benefit from dual therapy involving CDK4/6 inhibitors and agents targeting S6K1 or its upstream regulators.

Keywords: Breast cancer, CDK4/6 inhibitors, Drug resistance, Circulating tumour DNA, S6K1

How to Cite This Article: Miller JM, Fernandez KC, Moore PI, Smith OG, Sharma A, Tanaka A. S6K1 Amplification Drives Primary Resistance to CDK4/6 Inhibitors via c-Myc Pathway Activation in Estrogen Receptor–Positive Breast Cancer. Asian J Curr Res Clin Cancer. 2025;5(1):157-76. https://doi.org/10.51847/MUGZdK6vZB

Introduction

Breast cancer remains the leading malignancy among women globally, with an estimated 2,724,000 new diagnoses annually in China alone [1–3]. The ER-positive, HER2-negative subtype predominates, comprising over 60% of metastatic cases [4]. Agents targeting cyclin-dependent kinases 4 and 6 (CDK4/6), such as palbociclib, ribociclib, and abemaciclib, have dramatically extended progression-free and overall survival when paired with endocrine therapy in ER+ HER2− metastatic disease [5–8]. Consequently, this combined approach has emerged as the primary therapeutic strategy for affected patients.

Nevertheless, resistance to treatment limits long-term benefits for many individuals with ER+ HER2− metastatic breast cancer. A subset experiences no meaningful response to CDK4/6 inhibitors, progressing rapidly—often within three months—a phenomenon known as primary resistance. Identifying predictive markers for such resistance is essential to guide optimal therapy selection and minimize unnecessary toxicity from ineffective palbociclib use. Prior biomarker efforts in major phase III trials, relying mostly on archival tumor samples, have not yielded reliable predictors of response to palbociclib-endocrine combinations [9, 10]. Challenges include the difficulty of acquiring biopsy material from metastatic lesions in advanced disease, coupled with the fact that analysis of a single site may miss the full spectrum of tumor heterogeneity. In contrast, ctDNA profiling offers a noninvasive means to capture comprehensive genomic alterations across multiple metastatic deposits [11–14].

To address this, ctDNA analysis was applied to a clinical cohort of ER+ HER2− metastatic breast cancer patients **(Figure 1a)** to uncover predictors of primary resistance to CDK4/6 inhibitors. The leading candidate was then corroborated in a distinct patient group **(Figure 1b).** Cell-based studies elucidated the mechanistic role of the identified alteration in driving resistance to CDK4/6 blockade. Finally, patient-derived organoid and xenograft experiments **(Figures 1c and 1d)** informed potential strategies to circumvent primary resistance.

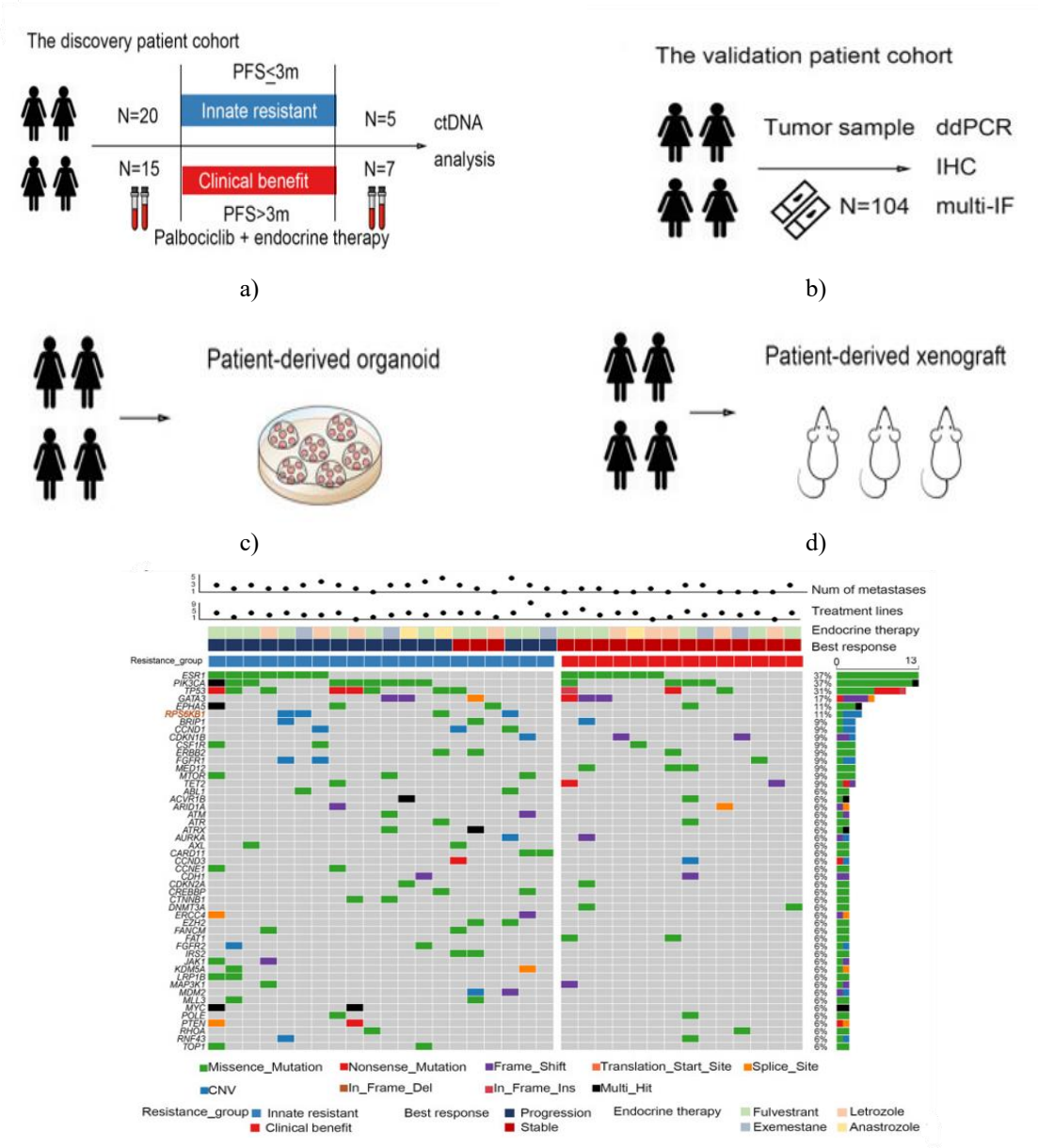

Figure 1. Investigation into the primary genetic factors contributing to primary resistance against CDK4/6 inhibitors involved examining circulating tumor DNA (ctDNA) obtained from individuals diagnosed with breast cancer.

a-d) Diagrammatic representation of the research framework and processing steps. PFS: progression-free survival. ctDNA: circulating tumor DNA. ddPCR: droplet digital PCR. IHC: immunohistochemistry. Multi-IF: multiplex immunofluorescence.

e) Distribution of frequently mutated genes in blood samples from the initial patient group. The figure displays cases exhibiting primary resistance or therapeutic response after palbociclib therapy, including details on metastatic sites, prior treatment regimens, and endocrine agents combined with palbociclib. Amplification of S6K1 (also known as RPS6KB1) was detected in three cases showing primary resistance to palbociclib, but absent in those demonstrating therapeutic response.

Materials and Methods

Patients and sample collection

Between May 2016 and November 2019, 186 individuals attended the Cancer Hospital, Chinese Academy of Medical Sciences, and received prescriptions for palbociclib. Of these, 36 consented to provide blood samples for ctDNA evaluation prior to starting therapy, forming the initial exploratory group for this research (NCC Protocol #1787). A separate confirmatory group included patients with ER-positive breast cancer who had archived tissue specimens in the institutional biobank. This encompassed 104 cases overall, with 37 having undergone palbociclib therapy. All blood and tissue specimens were collected following proper informed consent documentation. Patient records were gathered and examined via electronic health records accessed from the China National Cancer Center database. Standard computed tomography (CT) imaging was conducted as part of regular patient management at the Cancer Hospital, Chinese Academy of Medical Sciences. Tumor response assessments according to RECIST 1.1 criteria were carried out by a qualified radiologist experienced in oncology measurements. The research received approval from the Ethics Committee of the Cancer Institute and Hospital, Chinese Academy of Medical Sciences (12-123/657). Informed consent was obtained from every participant.

Progression-free survival (PFS) was calculated as the time from palbociclib initiation until documented disease progression, as assessed by clinicians using imaging data. Therapeutic response was classified as PFS exceeding 3 months, while primary resistance was classified as PFS of 3 months or less after starting palbociclib. The 3-month threshold was selected due to the advanced prior treatment history in most cases and alignment with earlier research [15]. Baseline patient features were grouped and statistically compared via Fisher's exact tests.

Sequencing and bioinformatics analysis

Blood-derived DNA from 36 individuals with metastatic breast cancer underwent targeted sequencing with a panel covering 1021 oncology-relevant genes [16]. Specimen processing adhered to established protocols and vendor guidelines. DNA isolation, library construction, capture enrichment, and sequencing followed previously outlined methods [17]. Identification of somatic single nucleotide variants employed the GATK toolkit version 3.4-46-gbc02625, followed by variant filtering. Copy number alterations were detected using CONTRA software version 2.0.8, with paired peripheral blood leukocytes serving as normal controls.

Whole exome sequencing data of patients with MBC from the INSERM cohort [18] and the Metastatic Breast Cancer Project (https://www.mbcproject.org/, a project of Count Me In (https://joincountmein.org/)) [19], and patients with primary breast invasive carcinoma from The Cancer Genome Atlas (TCGA, Firehose Legacy) were used to analyse the prevalence of S6K1 gene amplification in breast cancer using cBioPortal (http://www.cbioportal.org/). For pan-cancer analysis, the gene alteration data involved 10,967 tumour samples from 32 TCGA PanCancer Atlas Studies was obtained from cBioPortal. The RNA-seq data in 17 cancer types from TCGA was downloaded from the Human Protein Atlas.

Differential gene expression analysis involved retrieving count-based expression data from the BRCA dataset via the PanCancer Atlas resource. Fold-change calculations for high versus low S6K1 expression groups were performed using the EdgeR package in R [20]. Gene Set Enrichment Analysis (GSEA) was conducted with the clusterProfiler package to pinpoint key genes and shared pathways [21]. Statistical tests included t-tests, Fisher's exact tests, and Spearman correlations. Significance was set at a two-sided P value below 0.05. All computations utilized R version 3.6.1.

For RNA sequencing experiments, total RNA was isolated from MCF-7 cells treated with S6K1-specific siRNA or scrambled control siRNA using TRIzol Reagent (Invitrogen). Subsequently, 2 μg of RNA was processed for library creation with the KCTM Stranded mRNA Library Prep Kit (Wuhan Seqhealth Co., Ltd., China) per the

protocol. Amplified fragments ranging from 200 to 500 base pairs were selected, quantified, and sequenced on the Novaseq 6000 platform (Illumina) in paired-end 150 bp mode.

Immunohistochemistry (IHC)
Formalin-fixed paraffin-embedded (FFPE) tissue samples from breast cancer patients were obtained from the Cancer Hospital, Chinese Academy of Medical Sciences. Among 104 specimens, 61 originated from metastatic sites and 43 from primary tumours. Sections were incubated overnight at 4 °C with a polyclonal antibody against S6K1 (1:1000 dilution; Servicebio, Cat# GB111181). Subsequent incubation with secondary antibody (1:200 dilution; Servicebio, Cat# GB23303) was carried out for 50 min at room temperature. To exclude non-specific staining, each run included a negative control slide in which the primary antibody was substituted with 10% normal goat serum. Evaluation of staining was conducted by pathologists blinded to both sample identity and clinical outcomes. Cytoplasmic staining intensity was scored as follows: 0 (absent), 1 (weak), 2 (moderate), or 3 (strong). The percentage of positively stained cells was scored as: 0 (0–5%), 1 (6–25%), 2 (26–50%), 3 (51–75%), or 4 (76–100%). The final immunoreactivity score was calculated by multiplying the intensity score by the extent score, yielding values between 0 (lowest) and 12 (highest). Patients were stratified into high-expression (score ≥6) and low-expression (score <6) groups. Survival curves between groups were compared using the log-rank test.

Droplet digital PCR (ddPCR)
Copy number variation (CNV) of the S6K1 gene in FFPE samples was quantified using a custom multiplex droplet digital PCR assay on the OS-300 platform (Dawei Biotech, China) with OsciDrop technology [22]. Paraffin was removed using deparaffinization solution, and genomic DNA was isolated with the GeneRead DNA FFPE Kit (Qiagen N. V., Germany). DNA was eluted in 60 µL Buffer ATE (Qiagen), measured on a NanoDrop One spectrophotometer (Thermo Fisher Scientific, USA), and adjusted to 10 ng/µL with nuclease-free water. Each 25 µL reaction contained 12.5 µL 2X ddPCR Multiplex Supermix (Dawei Biotech), 2.5 µL primer/probe mix for S6K1 CNV (Dawei Biotech), 0.65 µL DNA polymerase, 2.5 µL template DNA, and 6.85 µL nuclease-free water. Amplification conditions were: 95 °C for 5 min, followed by 45 cycles of 94 °C for 20 s and 58 °C for 60 s, with a final hold at 25 °C.
To establish a threshold for S6K1 amplification, the mean copy-number ratio of S6K1 relative to the reference locus CEP17 was calculated from 26 breast cancer samples showing low S6K1 expression by IHC (score <6). Positive amplification was defined as a ratio exceeding the mean plus one standard deviation (threshold = 3.546).

Multiplex immunofluorescence (multi-IF)
To simultaneously assess S6K1 and cell cycle-associated protein levels in tumours, FFPE sections from ER+HER2− breast cancer patients in the validation cohort who received palbociclib were analysed by multiplex immunofluorescence and multispectral imaging. Antibodies used targeted cyclin E1 (Abcam, Cat# ab135380), cyclin D1 (CST, Cat# 2978 T), phospho-Rb (CST, Cat# 8516 T), S6K1 (CST, Cat# 2708 T), CDK4 (Proteintech, Cat# 11026-1-AP), and CDK6 (Abcam, Cat# ab124821). Primary antibodies were applied sequentially, followed by secondary antibody incubation and tyramide signal amplification (TSA). After completion of antigen labelling, nuclei were counterstained with DAPI. Slides were scanned on the Mantra System (PerkinElmer), acquiring fluorescence spectra at 20-nm intervals from 420 to 720 nm under identical exposure settings. Individual images were compiled into a composite stack. Spectral signatures of tissue autofluorescence and each fluorophore were derived from unstained and single-stained control slides. A spectral library for multispectral unmixing was constructed using inForm software (Version 2.4, PerkinElmer), and final images were generated with autofluorescence subtracted. Spearman correlation was applied to evaluate relationships between S6K1 and cell cycle marker expression, while the Mann-Whitney test was used to compare proportions of defined cellular subpopulations.

Cell culture and drugs
T47D and MCF-7 breast cancer cell lines, sourced from the American Type Culture Collection (ATCC), were cultured in DMEM (Cell Technologies) supplemented with 10% fetal bovine serum at 37 °C in a 5% CO_2 humidified incubator. Both lines were authenticated by short tandem repeat (STR) profiling. Palbociclib (HYA0065) and rapamycin (HY-10219) were obtained from MedChemExpress (MCE).

Cell proliferation and drug sensitivity assays

Real-time monitoring of cell proliferation was performed using the xCELLigence RTCA-MP system (Acea Biosciences/Roche Applied Science). MCF-7 cells (3×10^3 per well) or T47D cells (1×10^4 per well) were seeded in E-Plate 96 microtiter plates (Roche Applied Science), placed in the RTCA-MP station, and incubated under standard conditions. Cell index, reflecting electrical impedance changes, was recorded automatically every 15 min. For drug sensitivity experiments, cells were first allowed to adhere and grow for the specified duration, after which medium was replaced with varying concentrations or combinations of compounds.

Additional assessment of drug response employed CCK-8 and colony formation assays. In the CCK-8 assay, MCF-7 or T47D cells were seeded in 96-well plates, treated with escalating doses of palbociclib for 5 days starting 12 h after plating, and then analysed according to the CCK-8 kit protocol (NCM Biotech). For colony formation, cells were seeded in 12-well plates and exposed to palbociclib alone or combined with rapamycin. After ten days, colonies were fixed and visualised by crystal violet staining.

Western blotting and antibodies

Whole-cell lysates from breast cancer cell lines were separated by 10% SDS-PAGE and electrotransferred onto PVDF membranes. Membranes were blocked in 5% non-fat milk and then probed with primary antibodies overnight at 4 °C, followed by incubation with secondary antibodies for 1 h at room temperature. The primary antibodies employed were: S6K1 (Proteintech, Cat# 14485-1-AP), cyclin D1 (Proteintech, Cat# 60186-1-1 g), cyclin E1 (Abcam, Cat# ab33911), phospho-Rb (Abcam, Cat# ab109399), CDK2 (Proteintech, Cat# 10122-1-AP), CDK4 (Santa Cruz Biotechnology, Cat# sc-260), CDK6 (CST, Cat# 3136S), c-Myc (CST, Cat# 5605S), β-Actin (CST, Cat# 3700S), and GAPDH (Proteintech, Cat# 60004-1-Ig).

Small interfering RNA transfection and lentiviral infection

Cells were transfected with S6K1-specific siRNAs (RiboBio #stB0004595A: GATGAGAAGTGGCCACAAT; #stB0004595B: GGACGCTGGAGAAGTTCAA; #stB0004595C: GAGTTGGACCATATGAACT) or scrambled control siRNA using Lipofectamine 2000 (Invitrogen) according to the manufacturer's protocol.

To generate a stable S6K1-overexpressing T47D cell line, HEK293T cells were utilised for packaging S6K1-encoding lentivirus. The resulting viral supernatant was harvested and mixed 1:1 with T47D culture medium, followed by puromycin selection of transduced cells.

Reverse transcription-quantitative polymerase chain reaction (RT-qPCR)

Total RNA from breast cancer cells was extracted using TRIzol reagent (Invitrogen) and converted to cDNA with M-MLV reverse transcriptase (Promega). Quantitative PCR was conducted with BrightGreen 2X qPCR MasterMix (abm) on a CFX96 Real-Time System (Bio-Rad), with GAPDH as the normalisation control. Primer sequences were as follows: S6K1 forward 5′-GCCTCCCTACCTCACACAAG-3′, reverse 5′-CCACCTTTCGAGCCAGAAGT-3′; c-Myc forward 5′-GGCTCCTGGCAAAAGGTCA-3′, reverse 5′-CTGCGTAGTTGTGCTGATGT-3′; cyclin E1 forward 5′-GCCAGCCTTGGGACAATAATG-3′, reverse 5′-CTTGCACGTTGAGTTTGGGT-3′; GAPDH forward 5′-GCTGAGAACGGGAAGCTTGT-3′, reverse 5′-GCCAGGGGTGCTAAGCAGTT-3′.

Cell cycle analysis

Cells were harvested, washed in PBS, and fixed in 70% ethanol overnight at −20 °C. After PBS washing, cells were incubated with 500 μL PI/RNase Staining Buffer (BD Biosciences) for 15 min at 37 °C and subsequently analysed by flow cytometry (BD Biosciences).

Chromatin immunoprecipitation (ChIP)

ChIP experiments were performed using the Pierce Magnetic ChIP Kit (Thermo Fisher Scientific) according to the provided protocol. Chromatin from MCF-7 cells was digested and incubated with anti-c-Myc antibody (CST, Cat# 9402), followed by capture with magnetic beads. Purified immunoprecipitated DNA was analysed by qPCR for the CCNE1 promoter using the following primer sets:

CCNE1-promoter-1 (P1) forward 5′-AAGGACTTAGCCCAGTGCTG-3′, reverse 5′-CATCCTGTGCCCGTTAGGAAT-3′; CCNE1-promoter-2 (P2) forward 5′-

GTCAGAAAGGTCTTCAGAGAGCC-3′, reverse 5′-TGTCCATTCATCCGTCAGTGC-3′; CCNE1-promoter-3 (P3) forward 5′-CCACACATCCCCTTGGCTCA-3′, reverse 5′-GCGCGGGTGGAATGTAAACA-3′.

Luciferase reporter assay

The pGL3-CCNE1-promoter construct was generated by cloning the CCNE1 promoter region (−1 to −2000 bp) into the pGL3-basic vector. MCF-7 cells were co-transfected with either pGL3-CCNE1-promoter or pGL3-basic control, together with pRL-TK Renilla vector and either S6K1-targeting or control siRNAs, using Lipofectamine 2000 (Invitrogen). Cells were lysed, and firefly and Renilla luciferase activities were measured using the Dual Luciferase Reporter Assay System (Promega). Renilla activity served as the internal normalisation control for firefly activity.

Patient-derived organoid (PDO) study

Patient-derived breast cancer organoids were generated according to established protocols [23]. Tumour specimens were collected from participants in a clinical trial (NCT03544047) with informed consent. Tissues were mechanically minced and enzymatically digested with collagenase (Sigma-Aldrich, 1 mg/ml) and dispase (Sigma-Aldrich, 1 mg/ml) for 1–2 h at 37 °C. Isolated cells were resuspended in growth factor-reduced Matrigel (Corning) on ice, plated, and allowed to solidify at 37 °C for 30 min. Solidified domes were overlaid with complete breast cancer organoid medium (advanced DMEM/F12 with supplements as detailed by Sachs *et al*. [23]). Organoids were passaged bi-weekly using TrypLE digestion (Gibco).

For drug testing, organoids were seeded in 96-well plates with Matrigel for 2 days, then exposed to serial dilutions of palbociclib alone or combined with the mTOR inhibitor everolimus for 96 h. Viability was assessed using CellTiter-Glo® (Promega). Dose-response curves were constructed in GraphPad Prism (version 8.0). Synergy between palbociclib and everolimus was evaluated via dose-response matrix analysis [24], with Bliss synergy scores computed and visualised using the SynergyFinder R package [24, 25].

Patient-derived xenograft (PDX) study

A tumour sample from a breast cancer patient exhibiting S6K1 gene amplification was sourced from the commercial provider Crown Bioscience in China. Tissue fragments weighing approximately 20–30 mg were subcutaneously implanted into 9 NOD.SCID mice. All animal procedures were conducted in compliance with protocols approved by the institutional animal care and use committee. Once tumours reached a volume of ≥150 mm^3, mice were randomly assigned to one of three treatment arms: (1) vehicle control, (2) palbociclib (50 mg/kg, daily oral gavage), or (3) palbociclib combined with rapamycin (6 mg/kg, daily intraperitoneal injection). Body weight and tumour dimensions (measured by calipers) were recorded twice per week. After four weeks of treatment, mice were euthanised, and excised tumours were processed into formalin-fixed paraffin-embedded (FFPE) blocks for immunohistochemical analysis. Staining was performed using antibodies directed against cyclin E1 (Abcam, Cat# ab135380), cyclin D1 (CST, Cat# 2978 T), phospho-Rb (CST, Cat# 8516 T), S6K1 (Servicebio, Cat# GB111181), and Ki67 (Servicebio, Cat# GB13030-M-2).

Statistical analysis

Statistical analyses were carried out as specified for each experiment. Unless otherwise indicated in the figure legends, data are presented as mean ± standard deviation (SD). Comparisons between two groups were performed using two-sided Student's t-test, except where another method is noted. For comparisons involving multiple groups, one-way ANOVA was applied when no data were missing, whereas a mixed-effects model was used in cases with missing values. Statistical significance was defined as $P < 0.05$, and analyses were conducted using GraphPad Prism software (denoted as **** $P < 0.0001$; *** $P < 0.001$; ** $P < 0.01$; * $P < 0.05$).

Results and Discussion

Patients and clinical characteristics

To identify somatic alterations linked to clinical resistance against CDK4/6 inhibitors in breast cancer, 36 patients with ER-positive, HER2-negative metastatic breast cancer (MBC) who were treated with palbociclib in combination with endocrine therapy were enrolled as the discovery cohort **(Figure 1a).** One patient withdrew from palbociclib after 4 weeks due to severe myelosuppression, leaving resistance status undetermined; subsequent ctDNA-based resistance analysis therefore encompassed the remaining 35 patients.

Among the 36 patients, 18 (50.0 percent) were treated with palbociclib plus fulvestrant, 10 (27.8 percent) with palbociclib plus letrozole, 5 (13.9 percent) with palbociclib plus exemestane, and 3 (8.3%) with palbociclib plus anastrozole. Prior to palbociclib, patients had received a median of 3 (range 0–8) lines of systemic therapy for metastatic disease. Only 4 patients (11.1%) received CDK4/6 inhibitor-containing regimens as first-line treatment for metastasis, while 19 (52.8%) had undergone at least 3 prior systemic lines. At the time of analysis, 32 patients had progressed on palbociclib therapy, whereas 3 remained on treatment. Fifteen patients derived clinical benefit, defined as progression-free survival exceeding 3 months, while 20 exhibited primary resistance (PFS ≤ 3 months). No statistically significant differences in clinical or pathological characteristics were observed between the clinical benefit (n = 15) and primary resistance (n = 20) groups.

Analysis of circulating tumor DNA (ctDNA) uncovers multiple pathways involved in resistance to palbociclib

In our discovery cohort, 47 plasma samples underwent ctDNA analysis with a comprehensive panel covering 1021 genes associated with cancer: 35 samples obtained prior to starting palbociclib therapy, and 12 samples taken following progression of disease **(Figure 1a).**

We first examined possible predictive markers of palbociclib resistance using ctDNA alterations detected in plasma samples collected before treatment initiation. Among the 35 pretreatment samples, 34 (97.1%) exhibited at least one somatic alteration in genes relevant to cancer, averaging 8 alterations per sample (range 0–24). The distribution of frequently altered genes (>5%) in individuals classified as having innate resistance versus those deriving clinical benefit is shown in **Figure 1e**. In agreement with earlier studies [12], the genes most commonly mutated in metastatic breast cancer (MBC) were ESR1, PIK3CA, and TP53. Mutations in ESR1 appeared in 13 cases (13/35, 37.1%), with D538G being the predominant variant (6/35), then Y537S (4/35) and L536H (3/35). PIK3CA mutations occurred in 13 cases (13/35, 37.1%), primarily H1047R (8/35) followed by E545K (3/35). TP53 mutations were present in 11 cases (11/35, 31.4%), with R213* as the top recurring change (2/35). Among the 20 individuals showing innate resistance to palbociclib, the highest mutation rates were again in PIK3CA (9/20, 45.0%), TP53 (8/20, 40.0%), and ESR1 (7/20, 35.0%). The specific mutation sites in these genes were comparable between patients with and without innate resistance.

Various activating alterations in the PI3K pathway were identified in 19 cases, involving genes such as PIK, S6K1, MTOR, PTEN, AKT, and TSC1. The prevalence of PI3K pathway changes was markedly greater in the innate resistance cohort (14/20, 70.0%) compared to the clinical benefit cohort (5/15, 33.3%; P = 0.044), indicating that dysregulated PI3K signaling may drive primary resistance to palbociclib. Of particular interest, alterations in S6K1 (4/20, 20.0%), CCND1 (3/20, 15.0%), and MTOR (3/20, 15.0%) were exclusively found in the innate resistance group and absent in patients achieving clinical benefit **(Figure 1e)**; pointing to their potential role in mediating innate resistance to palbociclib.

Paired ctDNA testing (baseline and post-progression) was performed for 12 patients. Marked changes in the genomic profile were observed between pretreatment and post-progression samples. Among the 7 patients who initially responded to palbociclib, 3 developed novel mutations post-progression: one in TSC2, one in PTEN, and one with emerging alterations in ESR1, RB1, and TP53. These findings implicate these genes in the development of acquired resistance to palbociclib.

Amplification of S6K1 drives palbociclib resistance in breast cancer patients

From the ctDNA evaluation in the discovery cohort, amplification of S6K1 (defined as copy number ≥2.5) was identified in 3 cases (3/20, 15.0%) with innate resistance at baseline, while absent in patients with clinical benefit (0/15), **(Figure 1e).** Analysis of co-occurrence patterns among frequently altered genes revealed mutual exclusivity between S6K1 and PIK3CA in the innate resistance subgroup. All three patients harboring baseline S6K1 amplification had received at least two prior lines of endocrine therapy for metastatic disease. Notably, S6K1 amplification was not observed in post-treatment plasma samples, even among those developing acquired resistance. Thus, S6K1 emerges as a promising marker for innate resistance mechanisms.

The S6K1 gene plays a key role in the PI3K pathway and is situated at chromosome 17q23. Examination of TCGA sequencing data indicated that elevated S6K1 amplification and mRNA expression are predominantly observed in breast cancer (P < 0.0001), **(Figures 2a and 2b).** Aggregated data from cBioPortal revealed S6K1 amplification in around 12% of breast cancer cases, chiefly in the estrogen receptor-positive subtype **(Figure 2c).** Rates were 14% in metastatic breast cancer and 11% in primary tumors. S6K1 amplification correlated with elevated mRNA levels, which in turn associated with increased protein expression in breast tumors. Aligning with our discovery

cohort, TCGA PanCancer Atlas data for breast cancer demonstrated mutual exclusivity between S6K1 and PIK3CA (P = 0.030, Log2 odds ratio = −0.679). In samples with high S6K1 expression from TCGA, 210 mRNAs were upregulated and 406 downregulated by ≥2-fold. Pathway enrichment in the high S6K1 group highlighted significant involvement of cell cycle processes. Using GEPIA on TCGA BRCA data, S6K1 expression strongly correlated with cell cycle gene transcripts, notably CCNE2 (P < 0.001, r = 0.50), RB1 (P < 0.001, r = 0.46), CDK2 (P < 0.001, r = 0.45), CCND1 (P < 0.001, r = 0.37), and CDK4 (P < 0.001, r = 0.24), **(Figure 2d)**. Analysis via Kaplan-Meier Plotter [26] indicated that elevated S6K1 expression predicted poorer relapse-free survival in breast cancer (hazard ratio = 1.31, P < 0.0001), with stronger effects in the ER-positive subset (hazard ratio = 1.34, P = 0.0013), **(Figure 2e).**

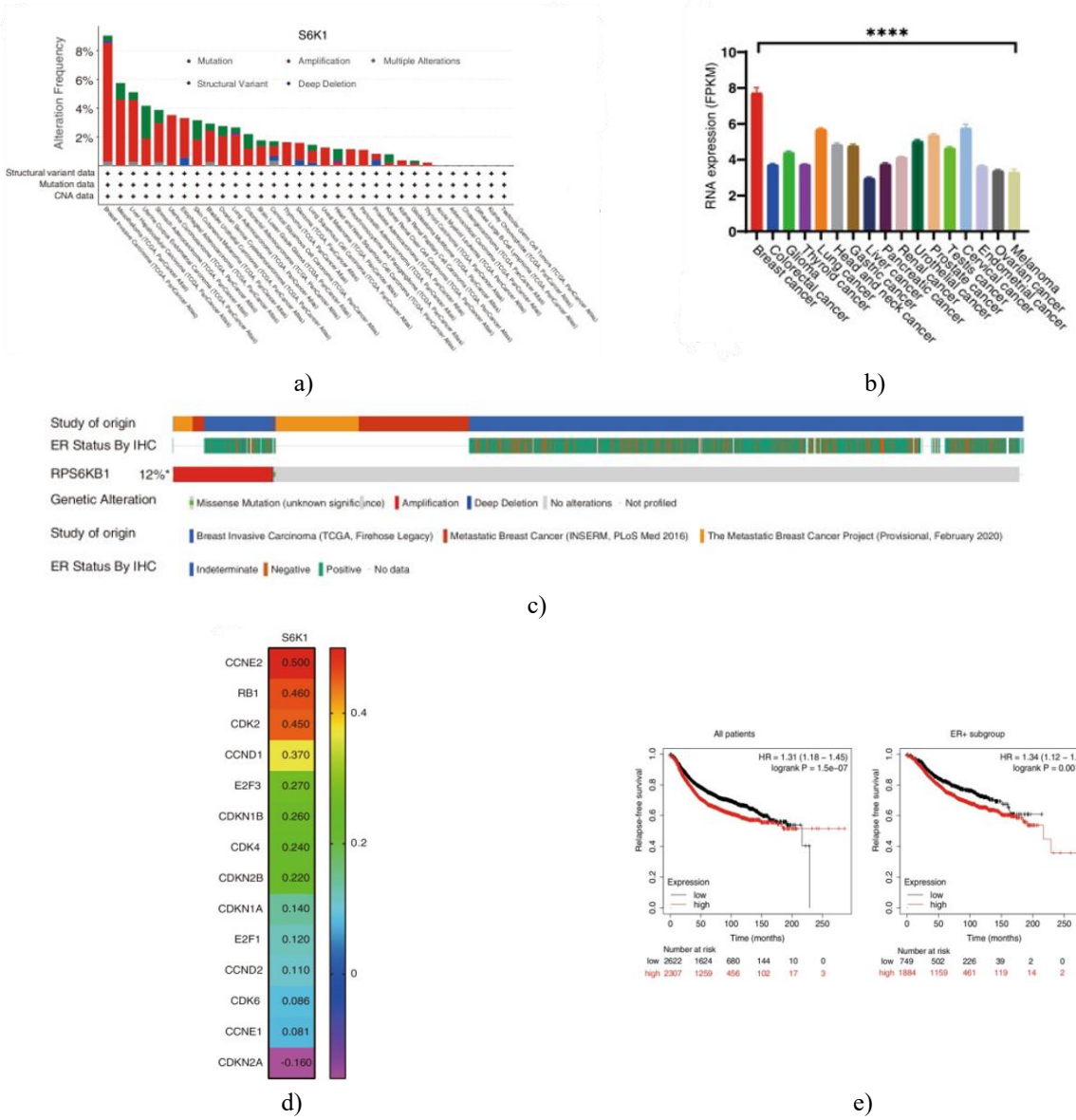

Figure 2. Genomic amplification of S6K1 is linked to adverse clinical outcomes in individuals diagnosed with breast cancer, as evidenced by data from open-access repositories.

a) The prevalence of genomic changes in the S6K1 gene among diverse cancer categories, based on a review of 10,967 tumor samples from the TCGA PanCancer Atlas collection retrieved through cBioPortal.

b) S6K1 mRNA expression in cases across multiple tumor entities from the TCGA collection, presented as median FPKM (Fragments Per Kilobase of exon per Million reads) units, acquired from the Human Protein Atlas. Results are displayed as mean ± standard error of the mean. Significance assessed via Kruskal-Wallis test. ****, P < 0.0001.

c) Notable amplification at the S6K1 gene locus primarily in estrogen receptor (ER)-positive breast cancer subtypes, per cBioPortal dataset.

d) Links between S6K1 mRNA quantities and cell cycle-associated gene expression in the breast invasive carcinoma (BRCA) patient group, derived from GEPIA platform analyses.

e) Kaplan-Meier curves depicting relapse-free survival probabilities for breast cancer cases categorized by S6K1 transcript levels, generated via the Kaplan-Meier Plotter resource.

Thereafter, we explored the connection between S6K1 status and palbociclib response in an independent group of 104 individuals with ER-positive metastatic breast cancer (MBC). S6K1 protein abundance was first measured through immunohistochemistry (IHC). **Figure 3a** illustrates overexpression of S6K1 in 15/104 (14%) specimens, characterized by IHC scores of 6-8. Of these patients, 37 received palbociclib therapy, with 29.7% (11/37) displaying high S6K1. Those with elevated S6K1 demonstrated considerably reduced progression-free survival relative to low-expression cases (median PFS 3.9 versus 15.6 months, hazard ratio = 3.0, 95% CI 1.0-8.8, P = 0.0072), **(Figure 3b).** Using droplet digital PCR (ddPCR), amplification of S6K1 was confirmed in 4/37 palbociclib-exposed patients **(Figure 3c).** Amplification occurred in 28.6% (2/7) of cases with inherent palbociclib resistance, versus only 4.3% (1/23) among those achieving therapeutic advantage.

Additionally, multiplex immunofluorescence (multi-IF) staining targeted various cell cycle proteins in samples stratified by S6K1 expression. Robust correlations emerged between S6K1 and cyclin E1 (r = 0.755, P = 0.006) alongside phosphorylated Rb (p-Rb) (r = 0.671, P = 0.020), **(Figures 3d and 3e).** Patients showing high S6K1 had markedly increased fractions of co-expressing cells for p-Rb/S6K1 (median 5.1% versus 0.8%, P < 0.0001) and cyclin E1/S6K1 (median 12.2% versus 1.6%, P < 0.0001) compared to low-S6K1 counterparts **(Figure 3f).**

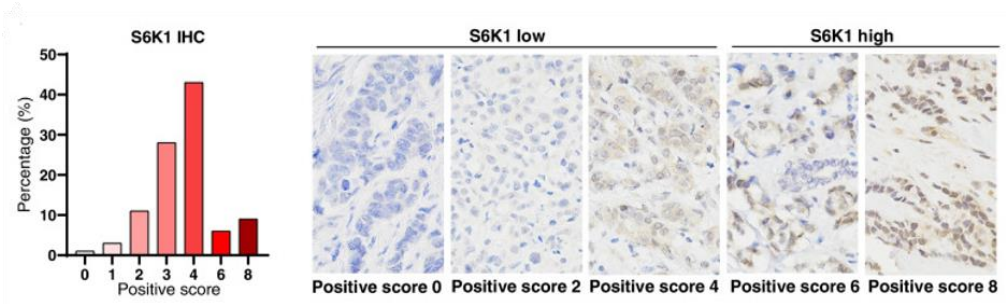

a)

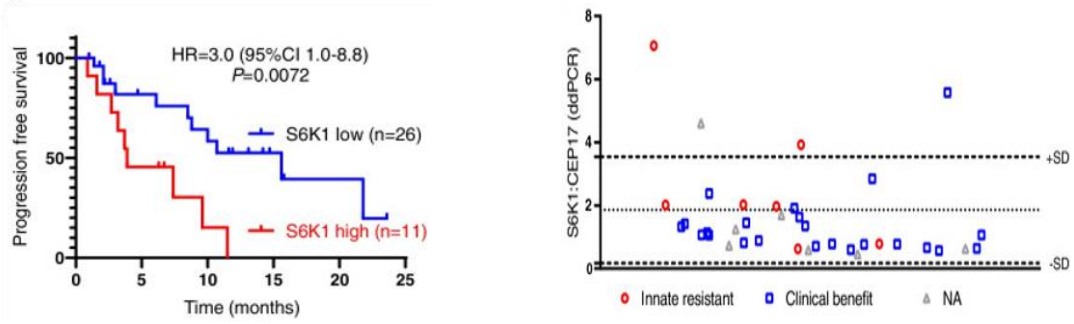

b) c)

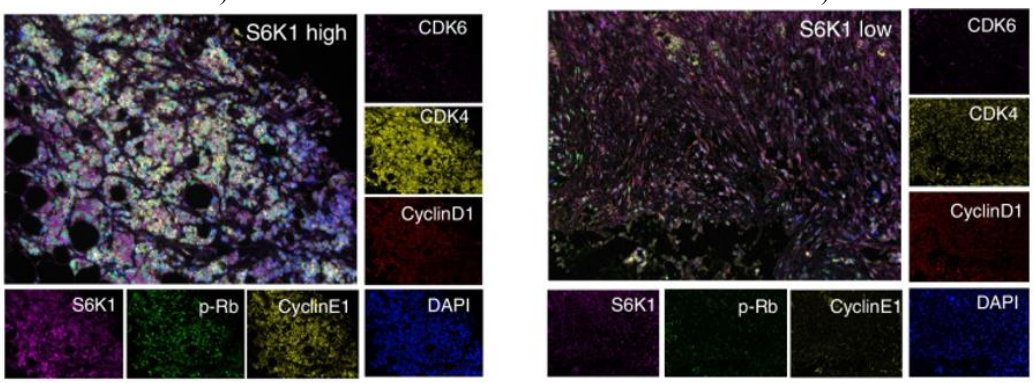

d)

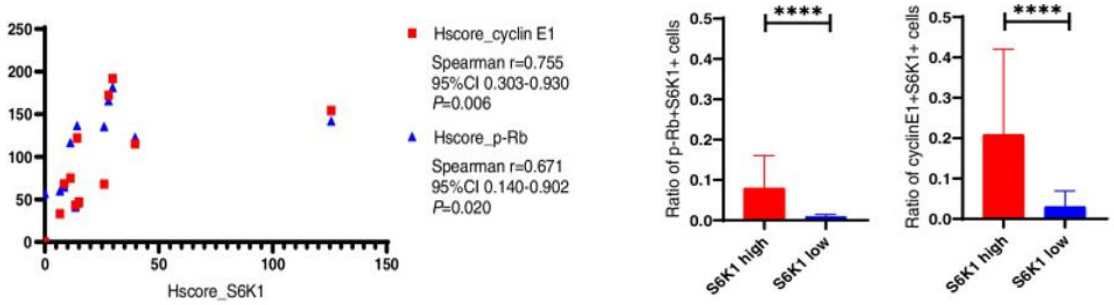

e) f)

Figure 3. Increased S6K1 expression is associated with palbociclib resistance in the independent validation cohort of patients.

a) S6K1 protein levels in breast cancer specimens were assessed using immunohistochemistry (IHC). Overexpression of S6K1 (defined by scores of 6–8) was detected in 15 out of 104 patients (14%).

b) Kaplan–Meier plots illustrating progression-free survival (PFS) among palbociclib-treated patients in the validation cohort, stratified by S6K1 expression level. Statistical significance determined by log-rank test.

c) Assessment of S6K1 gene copy number alterations through droplet digital PCR (ddPCR) analysis.

d) Representative multiplex immunofluorescence (multi-IF) images of tumor tissues from patients exhibiting high versus low S6K1 expression.

e) Strong positive correlations observed between S6K1 and both cyclin E1 and phosphorylated Rb (p-Rb) expression, based on multi-IF findings in patients with elevated S6K1.

f) Percentages of double-positive cells (p-Rb$^+$ S6K1$^+$ and cyclin E1$^+$ S6K1$^+$) in patients categorized by high or low S6K1 expression. Values shown as mean ± standard deviation. Significance evaluated using Mann-Whitney test. ****, P < 0.0001.

Taken together, these findings indicate that S6K1 gene amplification is frequently observed in breast cancer. High S6K1 expression appears to contribute significantly to palbociclib resistance mechanisms through modulation of the cell cycle pathway.

Overexpression of S6K1 drives cell proliferation and confers resistance to CDK4/6 inhibitors

We subsequently evaluated S6K1 levels in several breast cancer cell lines, including T47D, MCF-7, MDA-MB-468, and MDA-MB-231. Among these, MCF-7 cells exhibited the greatest S6K1 abundance at both mRNA and protein levels **(Figures 4a and 3b).** In agreement with data from the Cancer Cell Line Encyclopedia (CCLE) database [27], MCF-7 cells displayed substantially higher S6K1 transcript levels compared to most other breast cancer lines, attributable to elevated S6K1 gene copy number. Accordingly, we chose MCF-7 and T47D cells—both ER-positive/HER2-negative models—for in vitro studies to determine if S6K1 amplification underlies resistance to CDK4/6 inhibitors. As anticipated, MCF-7 cells demonstrated reduced sensitivity to palbociclib relative to T47D cells **(Figures 4c and 4d).** Moreover, siRNA-induced depletion of S6K1 in MCF-7 cells reinstated palbociclib responsiveness **(Figures 4e and 4f).** In contrast, stable overexpression of S6K1 via lentiviral transduction in T47D cells led to decreased palbociclib sensitivity compared to vector controls **(Figures 4g and 4h)**. Collectively, these data demonstrate that S6K1 overexpression resulting from gene amplification fosters resistance to palbociclib in ER-positive/HER2-negative breast cancer cells.

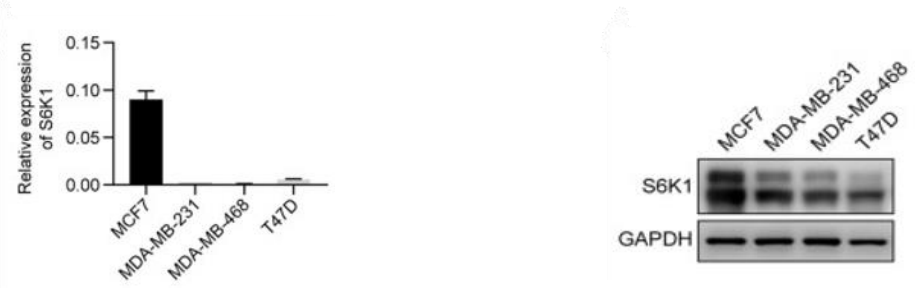

a) b)

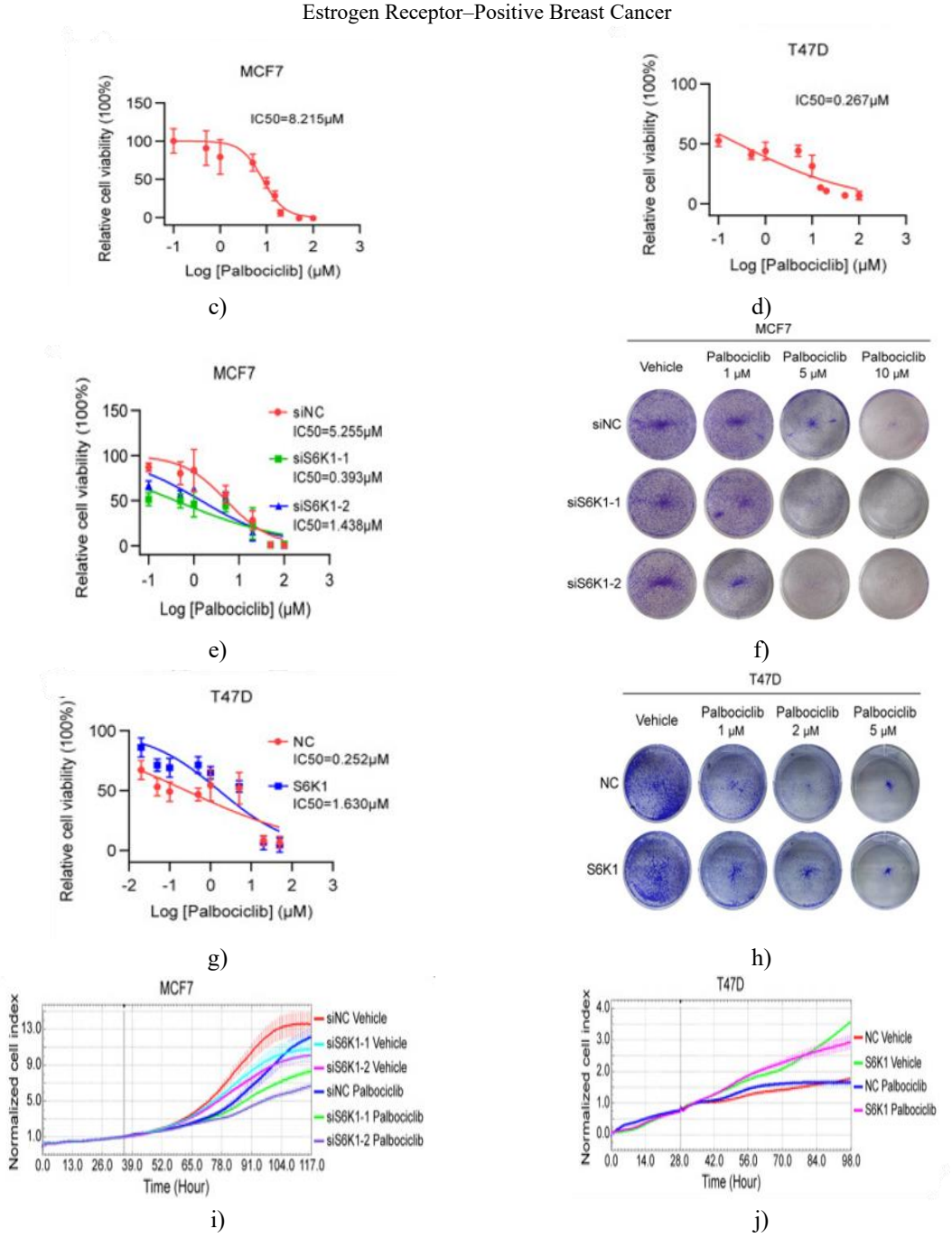

Figure 4. S6K1 drives resistance to palbociclib in models of breast cancer cells.

a, b) S6K1 levels were determined in four breast cancer cell lines (MCF-7, MDA-MB-231, MDA-MB-468, and T47D) by RT-qPCR (A) and western blot analysis (B).

c, d) MCF-7 (C) and T47D (D) cells were exposed to escalating concentrations of palbociclib for 5 days, after which cell viability was measured using the CCK-8 assay.

e, f) MCF-7 cells transfected with two targeted S6K1 siRNAs (siS6K1-1/−2) or a non-targeting control siRNA (siNC) were assessed for viability via CCK-8 assay (E) or clonogenic survival (F) following treatment with varying doses of palbociclib.

g, h) T47D cells stably overexpressing exogenous S6K1 or corresponding control cells underwent CCK-8 assay (G) or clonogenic assay (H) under the indicated palbociclib concentrations.

i, j) MCF-7 cells transfected with S6K1-specific siRNAs or control siRNA (I), as well as T47D cells with forced S6K1 expression or controls (J), were treated with or without palbociclib (10 μM for MCF-7; 1 μM for T47D). Real-time cell proliferation was monitored using the xCELLigence system.

In addition, we evaluated the impact of S6K1 on cell proliferation with the xCELLigence platform. Depletion of S6K1 in MCF-7 cells reduced proliferation both in the presence and absence of palbociclib **(Figure 4i).** In contrast, enforced S6K1 expression enhanced proliferation in T47D cells, including under palbociclib exposure (**Figure 4j).**

The c-Myc/cyclin E1 axis may underlie S6K1-mediated resistance to CDK4/6 inhibitors

We then explored the molecular basis by which S6K1 amplification contributes to resistance against CDK4/6 inhibitors. Since proliferation is tightly linked to cell cycle progression, we analyzed cell cycle phase distribution by flow cytometry. S6K1 knockdown resulted in a higher proportion of cells arrested in G1 phase, whereas S6K1 overexpression reduced the G1 fraction **(Figure 5a).**

To identify critical pathways modulated by S6K1, we performed transcriptome-wide RNA-sequencing (RNA-seq) on S6K1-depleted MCF-7 cells. This revealed 826 significantly differentially expressed genes (DEGs), comprising 486 upregulated and 340 downregulated transcripts ($P < 0.05$, $|\log2 \text{ fold change}| > 1$. Subsequent Kyoto Encyclopedia of Genes and Genomes (KEGG) and Gene Ontology (GO) enrichment analyses of the downregulated genes highlighted significant involvement of pathways related to cell proliferation and cell cycle regulation **(Figures 5b and 3c).** Consistent findings emerged from protein array profiling, reinforcing that S6K1 depletion in MCF-7 cells suppresses proliferative capacity.

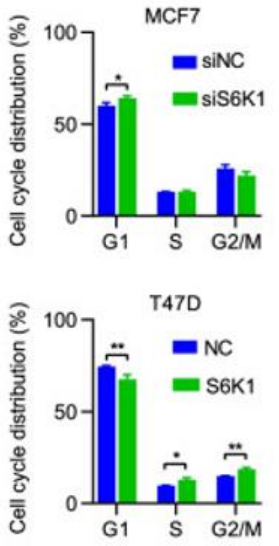

a)

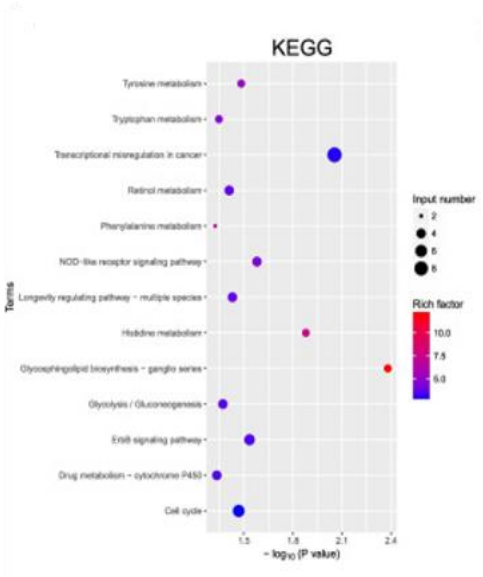

b)

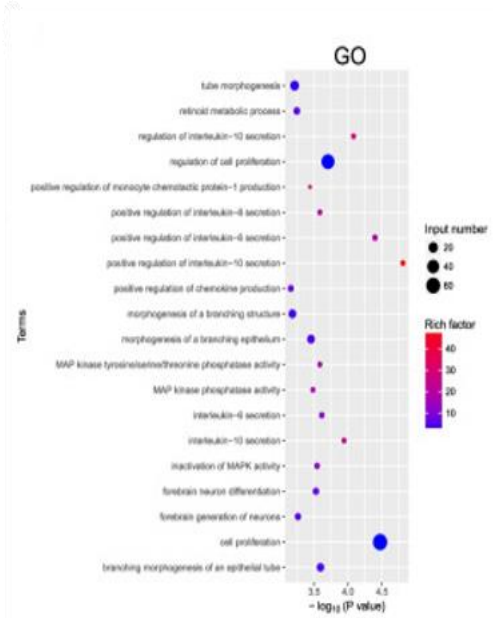

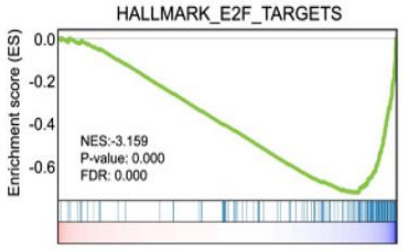

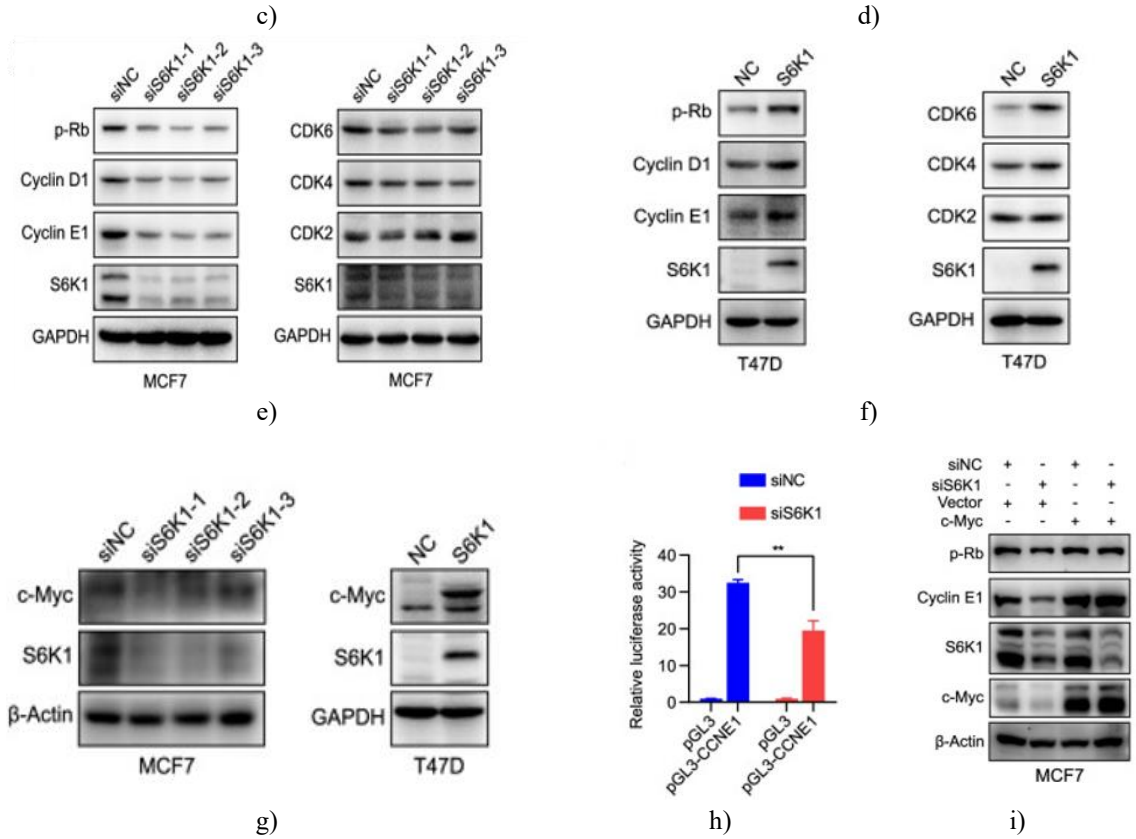

Figure 5. S6K1 enhances cell proliferation and palbociclib resistance by facilitating cell cycle progression.

a) Cell cycle phase distribution was evaluated by propidium iodide (PI) staining and flow cytometry in MCF-7 cells transfected with pooled S6K1 siRNA or control siRNA, as well as in T47D cells stably overexpressing S6K1 or vector controls. Statistical significance assessed by Student's t-test. *, $P < 0.05$; **, $P < 0.01$.

b, c) Kyoto Encyclopedia of Genes and Genomes (KEGG) pathway enrichment (B) and Gene Ontology (GO) functional annotation (C) performed on differentially expressed genes from RNA-seq data of S6K1-depleted MCF-7 cells.

d) Gene set enrichment analysis (GSEA) demonstrating significant enrichment of E2F-target and Myc-target gene signatures in S6K1-depleted MCF-7 cells.

e–g) Western blot analysis of protein extracts from MCF-7 cells transfected with the indicated siRNAs (E) and from T47D cells with forced S6K1 expression or controls (F, G). Blots were probed with antibodies targeting S6K1, cyclin D1, cyclin E1, CDK2, CDK4, CDK6, p-Rb, and c-Myc. GAPDH or β-Actin served as loading control.

h) Dual-luciferase reporter assay assessing transcriptional activity of the CCNE1 promoter in S6K1-depleted MCF-7 cells. Significance determined by Student's t-test. **, $P < 0.01$.

i) Western blot detection of cyclin E1 and p-Rb levels following re-introduction of c-Myc into S6K1-depleted MCF-7 cells.

Further GSEA on the RNA-seq dataset confirmed significant enrichment of gene sets associated with cell cycle phases and E2F targets **(Figure 5d)**. Of particular note, Myc-target gene sets were also markedly enriched **(Figure 5d),** suggesting that c-Myc pathway activation may drive the cell cycle acceleration induced by S6K1. Examination of key cell cycle regulators revealed that protein levels of CDK4, CDK6, cyclin D1, and cyclin E1, along with Rb phosphorylation, were reduced upon S6K1 knockdown **(Figure 5e)** and elevated in cells overexpressing S6K1 **(Figure 5f),** relative to respective controls.

In light of the GSEA findings and prior reports of S6K1-mediated translational activation of c-Myc [28–30], we assessed c-Myc protein abundance. c-Myc levels decreased in S6K1-depleted cells and increased in S6K1-overexpressing cells compared to controls **(Figure 5g).** Notably, cyclin E1 mRNA was substantially reduced following S6K1 depletion, whereas c-Myc transcript levels remained unchanged.

Since c-Myc has been shown to transcriptionally regulate cyclin E1 [31], we verified c-Myc occupancy at the cyclin E1 promoter in MCF-7 cells using chromatin immunoprecipitation (ChIP). To examine transcriptional

control of cyclin E1 by S6K1, a luciferase reporter driven by the cyclin E1 promoter was employed. Dual-luciferase assays indicated that S6K1 depletion significantly lowered promoter activity **(Figure 5h)**. A rescue experiment re-expressing c-Myc in S6K1-knockdown cells restored cyclin E1 and p-Rb levels **(Figure 5i).** Overall, these data demonstrate that S6K1 accelerates G1/S transition to promote proliferation. Mechanistically, S6K1 upregulates cell cycle regulators, particularly cyclin E1, primarily via activation of the c-Myc pathway.

Inhibition of S6K1 enhances palbociclib efficacy both in vitro and in vivo

Since S6K1 is a direct downstream effector of mTORC1 [32], we tested whether pharmacologic mTORC1 blockade could overcome palbociclib resistance using the clinically approved inhibitor rapamycin. In T47D cells engineered to overexpress S6K1, which conferred relative palbociclib resistance, co-treatment with rapamycin fully abrogated this resistance **(Figure 6a).** Comparable reversal was observed in MCF-7 cells **(Figure 6b)**. Furthermore, combining palbociclib with rapamycin in MCF-7 cells led to greater reduction in p-Rb and cyclin E1 levels than palbociclib monotherapy **(Figure 6c).**

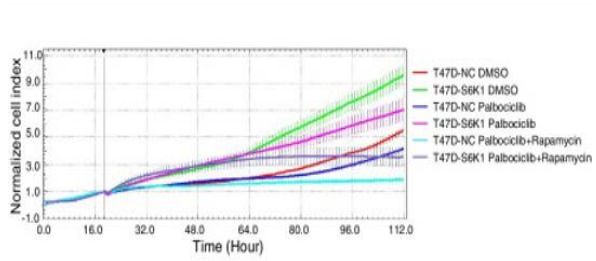

a)

b)

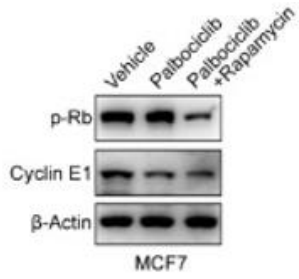

c)

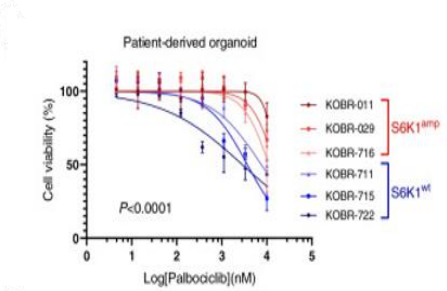

d)

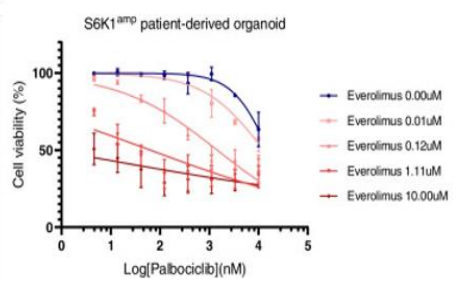

e)

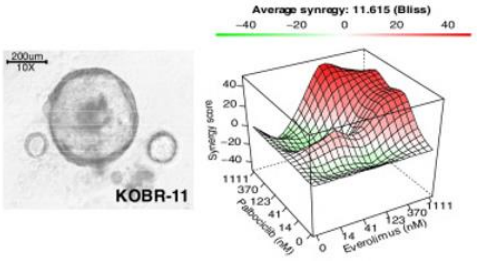

f)

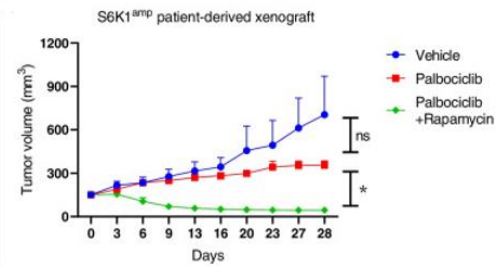

g)

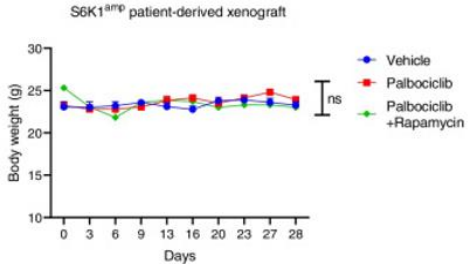

h)

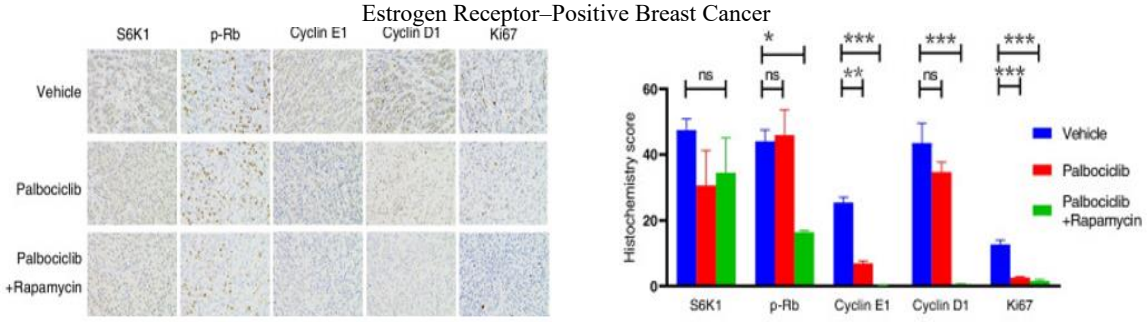

i) j)

Figure 6. mTOR inhibitors overcome palbociclib resistance both in vitro and in vivo.

a) Real-time proliferation monitoring via xCELLigence in T47D cells stably overexpressing exogenous S6K1 or control cells, treated with vehicle, palbociclib (100 nM), or palbociclib (100 nM) combined with rapamycin (500 nM, mTOR inhibitor).

b) Clonogenic survival assay in MCF-7 cells exposed to vehicle, palbociclib (5 μM), rapamycin (1 μM), or the combination.

c) Western blot analysis of cyclin E1 and p-Rb expression in MCF-7 cells treated as in B. β-Actin served as loading control.

d) Identification of three patient-derived organoids (PDOs) harboring S6K1 amplification (KOBR-011, −029, −716), which exhibited palbociclib resistance. PDOs with wild-type S6K1 (KOBR-711, −715, −722) were included as controls.

e) Co-administration of the mTOR inhibitor everolimus with palbociclib resulted in enhanced suppression of viability in S6K1-amplified PDOs.

f) Bliss synergy model depicting the combinatorial response landscape for palbociclib plus everolimus in the S6K1-amplified PDO KOBR-011.

g) Tumor volume measurements over 28 days in S6K1-amplified patient-derived xenografts (PDXs) treated with vehicle, palbociclib alone, or palbociclib combined with rapamycin. Values shown as mean ± SEM; significance by mixed-effects model. ns, not significant; *, $P < 0.05$.

h) Body weight monitoring in mice from the experiment described in G. Values shown as mean ± SEM; significance by mixed-effects model. ns, not significant.

i,j) Immunohistochemical staining of tumor sections from treated PDXs. (I) Representative images. (J) Quantification of staining intensity. Values shown as mean ± SEM; significance by one-way ANOVA. ns, not significant; *, $P < 0.05$; **, $P < 0.01$; ***, $P < 0.001$.

To further evaluate the therapeutic potential of combination treatment, we screened 32 breast cancer patient-derived organoids and identified three with S6K1 amplification (KOBR-011, KOBR-029, KOBR-716; incidence 9.4%, **(Figure 1c).** Relative to S6K1 wild-type PDOs (KOBR-711, KOBR-715, KOBR-722), the S6K1-amplified (S6K1^amp) organoids displayed marked palbociclib resistance ($P < 0.0001$), **(Figure 6d).** Palbociclib IC50 values were 15 μM, 15 μM, and 11 μM in S6K1^amp PDOs versus 7 μM, 4 μM, and 3 μM in wild-type counterparts. S6K1^amp PDOs also showed resistance to everolimus alone (IC50 23 μM and 13 μM). However, adding everolimus produced a pronounced leftward shift in the palbociclib dose-response curve and reduced IC50 values in S6K1^amp models **(Figure 6e).** At everolimus concentrations of 0.01 μM, 0.12 μM, 1.11 μM, and 10.00 μM, palbociclib IC50 dropped from 16 μM to 13 μM ($P = 0.436$), 1 μM ($P = 0.046$), 0.06 μM ($P = 0.046$), and 0.6 nM ($P = 0.024$), respectively. Bliss independence analysis in KOBR-011 revealed synergistic inhibition across multiple dose combinations, yielding an average synergy score of 11.6 **(Figure 6f).** These results indicate that palbociclib combined with everolimus achieves synergistic growth inhibition in S6K1-amplified breast cancer organoid models.

To validate these observations in vivo, we assessed the combination in an S6K1-amplified PDX model. Palbociclib monotherapy failed to suppress tumor growth ($P = 0.721$), **(Figure 6g),** confirming S6K1 amplification-mediated resistance in vivo. Adding rapamycin to palbociclib significantly reversed this resistance ($P = 0.021$, **(Figure 6g).** At day 28, tumor growth inhibition was 63% with palbociclib alone versus 119% with the combination ($P = 0.024$). No significant body weight reduction occurred with combination therapy ($P = 0.695$), **(Figure 6h),** suggesting acceptable tolerability. Immunohistochemistry of tumor sections confirmed high S6K1 expression in these models **(Figures 6i and 6j).** Palbociclib alone did not reduce p-Rb ($P = 0.962$) or cyclin D1

($P = 0.320$) levels, whereas the addition of mTOR inhibitor substantially lowered p-Rb ($P = 0.017$) and cyclin D1 ($P < 0.001$). Cyclin E1 was decreased by palbociclib monotherapy ($P = 0.002$) and further reduced by the combination ($P < 0.001$).

In summary, these findings highlight a pivotal role for S6K1 in mediating resistance to CDK4/6 inhibitors and demonstrate that mTOR inhibition can effectively overcome S6K1 amplification-driven resistance to palbociclib. To the best of our knowledge, this represents the first investigation to identify circulating tumor DNA (ctDNA)-detected S6K1 amplification as a marker of primary resistance to CDK4/6 inhibitors in individuals with ER-positive/HER2-negative metastatic breast cancer (MBC). Complementary in vitro and in vivo experiments indicate that resistance driven by S6K1 amplification is primarily mediated through c-Myc signaling pathways, leading to excessive activation of cyclins and CDKs. Consequently, patients harboring S6K1 amplification may not derive optimal benefit from CDK4/6 inhibitors combined with endocrine therapy. For this subgroup, targeting S6K1 via upstream mTOR inhibition could restore sensitivity to CDK4/6 inhibitors.

Analysis of ctDNA provides a comprehensive view of genomic alterations and is particularly valuable for tracking clonal dynamics in acquired resistance [12, 33]. Earlier efforts to identify predictors of primary resistance to CDK4/6 inhibitors using ctDNA employed smaller gene panels. For instance, in the PALOMA-3 trial, interrogation of mutations in 17 genes and copy number changes in 14 genes revealed associations between TP53 mutations or FGFR1 amplification and inherent palbociclib resistance [11]. The MONALEESA-7 trial linked CCND1 alterations to ribociclib resistance using a panel covering fewer than 600 genes [34]. The present work utilized the most extensive ctDNA panel reported to date—encompassing 1021 genes—to uncover biomarkers of innate resistance to CDK4/6 inhibitors. This approach successfully pinpointed S6K1 amplification as a predictive factor across two MBC patient cohorts. Given its prevalence (observed in 14% of MBC cases, predominantly ER-positive), routine ctDNA screening for S6K1 amplification prior to CDK4/6 inhibitor initiation could meaningfully inform treatment decisions in ER-positive MBC, sparing resistant patients from ineffective therapy while simultaneously detecting other actionable alterations.

Notably, S6K1 amplification was detected solely at baseline, prior to CDK4/6 inhibitor exposure, and was absent post-treatment with palbociclib. This pattern confirms that S6K1 amplification drives innate rather than acquired resistance. Large phase III trials examining ctDNA in the context of CDK4/6 inhibition have generally failed to identify robust resistance markers [34, 35], likely because they enrolled largely treatment-naïve or minimally pretreated patients (≤1 prior endocrine line). In contrast, our cohort comprised heavily pretreated individuals (median of 3 prior endocrine lines), where overall response rates to palbociclib are lower, potentially enriching for innate resistance mechanisms and facilitating biomarker discovery.

The PI3K/AKT/mTOR axis has been implicated in both early adaptation and acquired resistance to CDK4/6 inhibitors plus endocrine therapy [36–38]. CDK4/6 blockade can paradoxically activate AKT, promoting cyclin D1 accumulation [37]. Accordingly, aberrations in PI3K/AKT/mTOR components typically emerge after treatment initiation as acquired events [36, 39]. In our analysis, however, S6K1 amplification—a downstream alteration potentially mutually exclusive with PI3K mutations—was present pretreatment and linked to primary resistance. Thus, baseline ctDNA assessment of S6K1 status offers predictive utility that is unavailable for PI3K alterations associated with secondary resistance.

S6K1 activation enhances translation of specific mRNAs through phosphorylation of ribosomal protein S6 and eIF4B [40–42]. A prior melanoma study showed that S6K1 inhibition could overcome PIK3CA-driven CDK4/6 inhibitor resistance, though the underlying mechanism was unclear [43]. Here, in breast cancer models, we demonstrated that S6K1 overexpression elevates c-Myc protein, thereby transcriptionally upregulating cyclin E1, aligning with earlier reports [28–31]. Elevated cyclin E1 can bypass CDK4/6 inhibition by complexing with CDK2 to drive G1/S progression [10, 37, 44]. Consistent with this, pharmacologic mTOR inhibition sufficiently augmented palbociclib's antiproliferative effects, and PDX experiments validated that mTOR blockade reverses resistance while reducing cyclin E1 expression. These findings underscore S6K1 amplification's central role in cell cycle deregulation and CDK4/6 inhibitor resistance.

Patient-derived organoids (PDOs) faithfully mimic clinical drug responses and are increasingly employed for sensitivity testing across cancers, including breast cancer [23, 45]. We validated the S6K1–palbociclib resistance link in PDOs, observing marked resistance in amplified models akin to cell lines. Moreover, combining palbociclib with the mTOR inhibitor everolimus yielded superior growth inhibition versus either agent alone in S6K1-amplified PDOs, with Bliss analysis confirming synergy. Everolimus combined with endocrine agents has already demonstrated clinical benefit and acceptable tolerability [46, 47]. Trials exploring everolimus addition to

CDK4/6 inhibitor plus exemestane regimens in ER-positive/HER2-negative MBC are ongoing (NCT02732119, NCT01857193).

Conclusion

In conclusion, S6K1 amplification is a frequent event in ER-positive MBC, readily detectable via ctDNA, and strongly associated with primary resistance to CDK4/6 inhibitors. This genomic alteration drives c-Myc upregulation, consequent cyclin E1 overexpression, and accelerated cell cycle progression. Our data support combining mTOR inhibitors with CDK4/6 inhibitors as a promising strategy for ER-positive/HER2-negative breast cancers harboring S6K1 amplification.

Acknowledgments: None

Conflict of Interest: None

Financial Support: None

Ethics Statement: None

References

1. Chen W, Zheng R, Baade PD, Zhang S, Zeng H, Bray F, Jemal A, Yu XQ, He J. Cancer statistics in China, 2015. CA Cancer J Clin. 2016;66:115-32. doi: 10.3322/caac.21338.
2. Sung H, Ferlay J, Siegel RL, Laversanne M, Soerjomataram I, Jemal A, Bray F. Global cancer statistics 2020: GLOBOCAN estimates of incidence and mortality worldwide for 36 cancers in 185 countries. CA Cancer J Clin. 2021;71:209-49. doi: 10.3322/caac.21660.
3. Ma F, Wu J, Fu L, Li A, Lan B, Chen K, Di J, Jiang Y, Li J, Li N, et al. Interpretation of specification for breast cancer screening, early diagnosis, and treatment management in Chinese women. J Natl Cancer Center. 2021;1:97-100. doi: 10.1016/j.jncc.2021.07.003.
4. Gong Y, Liu YR, Ji P, Hu X, Shao ZM. Impact of molecular subtypes on metastatic breast cancer patients: a SEER population-based study. Sci Rep. 2017;7:45411. doi: 10.1038/srep45411.
5. Finn RS, Martin M, Rugo HS, Jones S, Im SA, Gelmon K, Harbeck N, Lipatov ON, Walshe JM, Moulder S, et al. Palbociclib and letrozole in advanced breast cancer. N Engl J Med. 2016;375:1925-36. doi: 10.1056/NEJMoa1607303.
6. Turner NC, Slamon DJ, Ro J, Bondarenko I, Im SA, Masuda N, Colleoni M, DeMichele A, Loi S, Verma S, et al. Overall survival with palbociclib and fulvestrant in advanced breast cancer. N Engl J Med. 2018;379:1926-36. doi: 10.1056/NEJMoa1810527.
7. Im SA, Lu YS, Bardia A, Harbeck N, Colleoni M, Franke F, Chow L, Sohn J, Lee KS, Campos-Gomez S, et al. Overall survival with ribociclib plus endocrine therapy in breast cancer. N Engl J Med. 2019;381:307-16. doi: 10.1056/NEJMoa1903765.
8. Fassl A, Geng Y, Sicinski P. CDK4 and CDK6 kinases: from basic science to cancer therapy. Science. 2022;375:eabc1495. doi: 10.1126/science.abc1495.
9. Finn RS, Liu Y, Zhu Z, Martin M, Rugo HS, Diéras V, Im SA, Gelmon KA, Harbeck N, Lu DR, et al. Biomarker analyses of response to cyclin-dependent kinase 4/6 inhibition and endocrine therapy in women with treatment-naïve metastatic breast cancer. Clin Cancer Res. 2020;26:110-21. doi: 10.1158/1078-0432.CCR-19-0751.
10. Turner NC, Liu Y, Zhu Z, Loi S, Colleoni M, Loibl S, et al. Cyclin E1 expression and palbociclib efficacy in previously treated hormone receptor-positive metastatic breast cancer. J Clin Oncol. 2019. doi: 10.1200/JCO.18.00925.
11. O'Leary B, Cutts RJ, Huang X, Hrebien S, Liu Y, André F, Loibl S, Loi S, Garcia-Murillas I, Cristofanilli M, et al. Circulating tumor DNA markers for early progression on fulvestrant with or without palbociclib in ER+ advanced breast cancer. J Natl Cancer Inst. 2021;113:309-17. doi: 10.1093/jnci/djaa087.

12. O'Leary B, Cutts RJ, Liu Y, Hrebien S, Huang X, Fenwick K, André F, Loibl S, Loi S, Garcia-Murillas I, et al. The genetic landscape and clonal evolution of breast cancer resistance to palbociclib plus fulvestrant in the PALOMA-3 trial. Cancer Discov. 2018;8:1390-403. doi: 10.1158/2159-8290.CD-18-0264.
13. Andre F, Su F, Solovieff N, Arteaga CL, Hortobagyi GN, Chia SKL, Neven P, Bardia A, Tripathy D, Lu Y-S, et al. Pooled ctDNA analysis of the MONALEESA (ML) phase III advanced breast cancer (ABC) trials. J Clin Oncol. 2020;38:1009. doi: 10.1200/JCO.2020.38.15_suppl.1009.
14. Sanz-Garcia E, Zhao E, Bratman SV, Siu LL. Monitoring and adapting cancer treatment using circulating tumor DNA kinetics: current research, opportunities, and challenges. Sci Adv. 2022;8:eabi8618. doi: 10.1126/sciadv.abi8618.
15. Wang DS, Liu ZX, Lu YX, Bao H, Wu X, Zeng ZL, Liu Z, Zhao Q, He CY, Lu JH, et al. Liquid biopsies to track trastuzumab resistance in metastatic HER2-positive gastric cancer. Gut. 2019;68:1152-61. doi: 10.1136/gutjnl-2018-316522.
16. Yi Z, Ma F, Rong G, Liu B, Guan Y, Li J, Sun X, Wang W, Guan X, Mo H, et al. The molecular tumor burden index as a response evaluation criterion in breast cancer. Signal Transduct Target Ther. 2021;6:251. doi: 10.1038/s41392-021-00662-9.
17. Yi Z, Rong G, Guan Y, Li J, Chang L, Li H, Liu B, Wang W, Guan X, Ouyang Q, et al. Molecular landscape and efficacy of HER2-targeted therapy in patients with HER2-mutated metastatic breast cancer. NPJ Breast Cancer. 2020;6:59. doi: 10.1038/s41523-020-00201-9.
18. Lefebvre C, Bachelot T, Filleron T, Pedrero M, Campone M, Soria JC, Massard C, Lévy C, Arnedos M, Lacroix-Triki M, et al. Mutational profile of metastatic breast cancers: a retrospective analysis. PLoS Med. 2016;13:e1002201. doi: 10.1371/journal.pmed.1002201.
19. Wagle N, Painter C, Krevalin M, Oh C, Anderka K, Larkin K, Lennon N, Dillon D, Frank E, Winer EP, et al. The metastatic breast cancer project: a national direct-to-patient initiative to accelerate genomics research. J Clin Oncol. 2016;34:LBA1519. doi: 10.1200/JCO.2016.34.18_suppl.LBA1519.
20. McCarthy DJ, Chen Y, Smyth GK. Differential expression analysis of multifactor RNA-Seq experiments with respect to biological variation. Nucleic Acids Res. 2012;40:4288-97. doi: 10.1093/nar/gks042.
21. Yu G, Wang LG, Han Y, He QY. clusterProfiler: an R package for comparing biological themes among gene clusters. Omics. 2012;16:284-7. doi: 10.1089/omi.2011.0118.
22. 22. Ye S, Li C, Zheng X, Huang W, Tao Y, Yu Y, Yang L, Lan Y, Ma L, Bian S, Du W. OsciDrop: a versatile deterministic droplet generator. Anal Chem. 2022;94(6):2918-25. doi: 10.1021/acs.analchem.1c04852.
23. Sachs N, de Ligt J, Kopper O, Gogola E, Bounova G, Weeber F, Balgobind AV, Wind K, Gracanin A, Begthel H, et al. A living biobank of breast cancer organoids captures disease heterogeneity. Cell. 2018;172:373-86.e310. doi: 10.1016/j.cell.2017.11.010.
24. He L, Kulesskiy E, Saarela J, Turunen L, Wennerberg K, Aittokallio T, Tang J. Methods for high-throughput drug combination screening and synergy scoring. Methods Mol Biol. 2018;1711:351-98. doi: 10.1007/978-1-4939-7493-1_17.
25. Zhao W, Sachsenmeier K, Zhang L, Sult E, Hollingsworth RE, Yang H. A new bliss Independence model to analyze drug combination data. J Biomol Screen. 2014;19:817-21. doi: 10.1177/1087057114521867.
26. Győrffy B. Survival analysis across the entire transcriptome identifies biomarkers with the highest prognostic power in breast cancer. Comput Struct Biotechnol J. 2021;19:4101–9. doi:10.1016/j.csbj.2021.07.014
27. Barretina J, Caponigro G, Stransky N, Venkatesan K, Margolin AA, Kim S, Wilson CJ, Lehár J, Kryukov GV, Sonkin D, et al. The cancer cell line encyclopedia enables predictive modelling of anticancer drug sensitivity. Nature. 2012;483:603–7. doi:10.1038/nature11003
28. Csibi A, Lee G, Yoon SO, Tong H, Ilter D, Elia I, Fendt SM, Roberts TM, Blenis J. The mTORC1/S6K1 pathway regulates glutamine metabolism through the eIF4B-dependent control of c-Myc translation. Curr Biol. 2014;24:2274–80. doi:10.1016/j.cub.2014.08.007
29. Foster DA, Yellen P, Xu L, Saqcena M. Regulation of G1 cell cycle progression: distinguishing the restriction point from a nutrient-sensing cell growth checkpoint(s). Genes Cancer. 2010;1:1124–31. doi:10.1177/1947601910392989
30. Ma XM, Blenis J. Molecular mechanisms of mTOR-mediated translational control. Nat Rev Mol Cell Biol. 2009;10:307–18. doi:10.1038/nrm2672

31. Obaya AJ, Mateyak MK, Sedivy JM. Mysterious liaisons: the relationship between c-Myc and the cell cycle. Oncogene. 1999;18:2934–41. doi:10.1038/sj.onc.1202749
32. Hay N, Sonenberg N. Upstream and downstream of mTOR. Genes Dev. 2004;18:1926–45. doi:10.1101/gad.1212704
33. Condorelli R, Spring L, O'Shaughnessy J, Lacroix L, Bailleux C, Scott V, Dubois J, Nagy RJ, Lanman RB, Iafrate AJ, et al. Polyclonal RB1 mutations and acquired resistance to CDK4/6 inhibitors in patients with metastatic breast cancer. Ann Oncol. 2018;29:640–5. doi:10.1093/annonc/mdx784
34. Bardia A, Su F, Solovieff N, Im SA, Sohn J, Lee KS, Campos-Gomez S, Jung KH, Colleoni M, Vázquez RV, et al. Genomic profiling of premenopausal HR+ and HER2- metastatic breast cancer by circulating tumor DNA and association of genetic alterations with therapeutic response to endocrine therapy and ribociclib. JCO Precis Oncol. 2021;5:PO.20.00445. doi:10.1200/PO.20.00445
35. Cristofanilli M, Turner NC, Bondarenko I, Ro J, Im SA, Masuda N, Colleoni M, DeMichele A, Loi S, Verma S, et al. Fulvestrant plus palbociclib versus fulvestrant plus placebo for treatment of hormone-receptor-positive, HER2-negative metastatic breast cancer that progressed on previous endocrine therapy (PALOMA-3): final analysis of the multicentre, double-blind, phase 3 randomised controlled trial. Lancet Oncol. 2016;17:425–39. doi:10.1016/S1470-2045(15)00613-0
36. Wander SA, Cohen O, Gong X, Johnson GN, Buendia-Buendia J, Lloyd MR, Kim D, Luo F, Mao P, Helvie K, et al. The genomic landscape of intrinsic and acquired resistance to cyclin-dependent kinase 4/6 inhibitors in patients with hormone receptor-positive metastatic breast cancer. Cancer Discov. 2020;10:1174–93. doi:10.1158/2159-8290.CD-19-1390
37. Herrera-Abreu MT, Palafox M, Asghar U, Rivas MA, Cutts RJ, Garcia-Murillas I, Pearson A, Guzman M, Rodriguez O, Grueso J, et al. Early adaptation and acquired resistance to CDK4/6 inhibition in estrogen receptor-positive breast cancer. Cancer Res. 2016;76:2301–13. doi:10.1158/0008-5472.CAN-15-0728
38. Michaloglou C, Crafter C, Siersbaek R, Delpuech O, Curwen JO, Carnevalli LS, Staniszewska AD, Polanska UM, Cheraghchi-Bashi A, Lawson M, et al. Combined inhibition of mTOR and CDK4/6 is required for optimal blockade of E2F function and long-term growth inhibition in estrogen receptor-positive breast cancer. Mol Cancer Ther. 2018;17:908–20. doi:10.1158/1535-7163.MCT-17-0537
39. O'Leary B, Hrebien S, Morden JP, Beaney M, Fribbens C, Huang X, Liu Y, Bartlett CH, Koehler M, Cristofanilli M, et al. Early circulating tumor DNA dynamics and clonal selection with palbociclib and fulvestrant for breast cancer. Nat Commun. 2018;9:896. doi:10.1038/s41467-018-03215-x
40. Saxton RA, Sabatini DM. mTOR signaling in growth, metabolism, and disease. Cell. 2017;168:960–76. doi:10.1016/j.cell.2017.02.004
41. Bahrami BF, Ataie-Kachoie P, Pourgholami MH, Morris DL. p70 ribosomal protein S6 kinase (Rps6kb1): an update. J Clin Pathol. 2014;67:1019–25. doi:10.1136/jclinpath-2014-202560
42. Holz MK, Ballif BA, Gygi SP, Blenis J. mTOR and S6K1 mediate assembly of the translation preinitiation complex through dynamic protein interchange and ordered phosphorylation events. Cell. 2005;123:569–80. doi:10.1016/j.cell.2005.10.024
43. Romano G, Chen PL, Song P, McQuade JL, Liang RJ, Liu M, Roh W, Duose DY, Carapeto FCL, Li J, et al. A preexisting rare PIK3CA(E545K) subpopulation confers clinical resistance to MEK plus CDK4/6 inhibition in NRAS melanoma and is dependent on S6K1 signaling. Cancer Discov. 2018;8:556–67. doi:10.1158/2159-8290.CD-17-0745
44. Chu C, Geng Y, Zhou Y, Sicinski P. Cyclin E in normal physiology and disease states. Trends Cell Biol. 2021;31:732–46. doi:10.1016/j.tcb.2021.05.001
45. Vlachogiannis G, Hedayat S, Vatsiou A, Jamin Y, Fernández-Mateos J, Khan K, Lampis A, Eason K, Huntingford I, Burke R, et al. Patient-derived organoids model treatment response of metastatic gastrointestinal cancers. Science. 2018;359:920–6. doi:10.1126/science.aao2774
46. Bachelot T, Bourgier C, Cropet C, Ray-Coquard I, Ferrero JM, Freyer G, Abadie-Lacourtoisie S, Eymard JC, Debled M, Spaëth D, et al. Randomized phase II trial of everolimus in combination with tamoxifen in patients with hormone receptor-positive, human epidermal growth factor receptor 2-negative metastatic breast cancer with prior exposure to aromatase inhibitors: a GINECO study. J Clin Oncol. 2012;30:2718–24. doi:10.1200/JCO.2011.39.0708
47. Jerusalem G, de Boer RH, Hurvitz S, Yardley DA, Kovalenko E, Ejlertsen B, Blau S, Özgüroglu M, Landherr L, Ewertz M, et al. Everolimus plus exemestane vs everolimus or capecitabine monotherapy for estrogen

receptor-positive, HER2-negative advanced breast cancer: the BOLERO-6 randomized clinical trial. JAMA Oncol. 2018;4:1367–74. doi:10.1001/jamaoncol.2018.2262